

Synthesis and crystal structure of triphenyltin and lead complexes with organic peroxides

Alexander G. Medvedev, Mikhail Yu. Sharipov, Dmitry A. Grishanov, Artur V. Eshtukov, Andrei V. Churakov, Ivan A. Buldashov, Pavel A. Egorov, Ovidia Lev and Petr V. Prikhodchenko

Experimental part

Materials and synthesis

Triphenyltin hydroxide (95%), triphenyltin chloride (95%), dimethyltin dichloride (97%), *tert*-butyl hydroperoxide (70% solution in water) and cumene hydroperoxide (80% solution in cumene) were purchased from Sigma-Aldrich. *tert*-butyl hydroperoxide (50% solution in diethyl ether) was prepared from water solution. All solvents were purified according to standard procedures and stored over molecular sieves. **Caution:** organotin(IV) compounds are highly toxic and require appropriate handling!

Synthesis of Ph₃SnOOCMe₂Ph (1). Triphenyltin hydroxide (0.2 g, 0.545 mmol) was dissolved in anhydrous benzene (30 mL). Cumene hydroperoxide solution (0.104 g, 0.545 mmol) was added to obtained solution of triphenyltin hydroxide and stirred for 5 min. The resulting was evaporated under vacuum at 50°C, then 50 mL of benzene was added to the product and repeated 3 times to remove residual water. The white crystalline triphenyltin(IV) cumene peroxide Ph₃SnOOCMe₂Ph was crystallized at room temperature from obtained viscous oil and rinsed with cold hexane (0.25 g, 92% yield, m.p. = 114°C). Anal. Calc. for C₂₇H₂₆O₂Sn₁ (1): OO (peroxide), 6.38; C, 64.70; H, 5.23; Sn, 23.68. Found: OO (peroxide), 6.32; C, 65.00; H, 5.33; Sn, 23.32. ¹H NMR (500.1 MHz, CD₃OD, rt) δ: 7.30-7.85 (m, 20H, Ph), 1.5 (s, 6H, CH₃); ¹³C NMR (125.8 MHz, CD₃OD, rt) δ: 147.1, 140.8, 137.8, 137.6, 137.5, 130.7, 130.6, 130.5, 130.0, 129.7, 129.5, 129.0, 127.9, 126.5, 84.1, 26.8.

Synthesis of Ph₃SnOOCMe₃ (2). Triphenyltin chloride (0.314 g, 0.815 mmol) was dissolved in anhydrous diethyl ether (9 mL). Anhydrous *tert*-butyl hydroperoxide 50% solution in diethyl ether (0.147 g, 0.815 mmol) was added to obtained solution of triphenyltin chloride and then dry ammonia gas was bubbled under the surface for 20 min precipitating ammonium chloride. The organic phase was separated by filtration and the filtrate evaporated under vacuum in a rotary evaporator. The white crystalline triphenyltin(IV) *tert*-butylperoxide, Ph₃SnOOCMe₃ was crystallized at -20°C from the obtained viscous oil and rinsed with cold hexane (0.30 g, 84% yield, m.p. = 68°C). Anal. Calc. for C₂₂H₂₄O₂Sn₁ (2): OO (peroxide), 7.30; C, 60.17; H, 5.51; Sn, 27.03. Found: OO (peroxide), 7.24; C, 60.48; H, 5.60; Sn, 26.85. ¹H NMR (500.1 MHz, CD₃OD, rt) δ: 7.3-7.8 (m, 15H, Ph), 1.2 (s, 9H, CH₃); ¹³C NMR (125.8 MHz, CD₃OD, rt) δ: 140.9, 137.6, 130.6, 129.7, 80.9, 26.3.

Synthesis of Ph₃PbOOCMe₂Ph (3). Triphenyllead hydroxide (0.09 g, 0.198 mmol) was dissolved in anhydrous benzene (50 mL). Cumene hydroperoxide solution (0.038 g, 0.198 mmol) was added to obtained solution of triphenyllead hydroxide and stirred for 5 min. The resulting was evaporated under vacuum at 15 °C, then 50 mL of benzene was added to the product and repeated 3 times to remove residual water. The white crystalline triphenyllead cumene peroxide Ph₃PbOOCMe₂Ph was crystallized at 4 °C from obtained viscous oil (0.10 g, 86% yield). Anal. Calc. for C₂₇H₂₆O₂Pb₁ (**1**): C, 54.99; H, 4.44. Found: C, 54.62; H, 4.59. ¹H NMR (500.1 MHz, CD₃OD, rt) δ: 7.21-7.91 (m, 20H, Ph), 1.5 (s, 6H, CH₃); ¹³C NMR (125.8 MHz, CD₃OD, rt) δ: 158.4, 147.0, 137.7, 137.6, 131.0, 130.6, 129.0, 127.9, 126.6, 84.1, 26.8.

X-ray diffraction studies were performed at the Centre of Shared Equipment of IGIC RAS. The crystallographic data for **1-3** have been deposited with the Cambridge Crystallographic Data Centre as supplementary publications under the CCDC numbers 2082383, 2082386, and 2107630, respectively.

Elemental analysis. Peroxide content was estimated by iodometry. Carbon and hydrogen content were determined using the Perkin-Elmer 2400 series II Analyzer (CHN), tin content was determined by gravimetric analysis.

X-ray powder diffraction measurements were performed on a D8 Advance diffractometer (Bruker AXS, Germany) with a goniometer radius of 280 mm. The powder samples were filled into low background quartz sample holders. The specimen weight was 0.2 g. XRD patterns in the range 5° to 40° 2θ were recorded at room temperature using CuKα radiation (λ=1.5418 Å) under the following measurement conditions: tube voltage of 40 kV, tube current of 40 mA, step scan mode with a step size 0.02° 2θ, and counting time of 0.5s/step. XRD patterns were processed by DiffracPlus software. High scanning speed caused by the low stability of **2** under X-ray irradiation at room temperature results in low signal/noise ratio.

Raman spectroscopy. The measurements were performed at room temperature with a Renishaw inVia Raman microscope. The incident light was 633 nm with a power of 0.1 mW. Regular spectra were acquired with a 50× objective.

FTIR spectra were recorded on a JASCO FT/IR-4600 spectrometer.

Differential scanning calorimetry (DSC) and **thermogravimetry (TGA)** were performed on differential scanning calorimeter, DSC-60 Plus, and differential thermal analyzer, DTG-60, respectively (Shimadzu). All experiments were carried out under argon flow at a heating rate of 5 °C/min.

¹H and ¹³C spectra were collected on a Bruker Avance-500 spectrometer at resonance frequency of 500.1 and 125.8 MHz, respectively. **¹¹⁹Sn NMR spectra** were collected on a Bruker Avance AV 600 spectrometer at resonance frequency of 223.8 MHz, respectively. Experiments were carried out at 25 °C.

Table S1. Selected bond distances (Å) and angles (°) in **1-3**.

1			
Sn(1)–O(1)	2.0201(16)	O(1)–Sn(1)–C(21)	106.80(8)
Sn(1)–C(21)	2.123(2)	O(1)–Sn(1)–C(31)	99.20(7)
Sn(1)–C(31)	2.126(2)	O(1)–Sn(1)–C(11)	109.44(7)
Sn(1)–C(11)	2.130(2)	O(2)–O(1)–Sn(1)	101.11(10)
O(1)–O(2)	1.484(2)	C(9)–O(2)–O(1)	107.83(14)
O(2)–C(9)	1.442(3)	Sn(1)–O(1)–O(2)–C(9)	132.56(13)
2			
Sn(1)–O(1)	2.014(2)	O(1)–Sn(1)–C(21)	109.12(12)
Sn(1)–C(21)	2.120(4)	O(1)–Sn(1)–C(11)	105.25(10)
Sn(1)–C(11)	2.132(3)	O(1)–Sn(1)–C(31)	101.59(11)
Sn(1)–C(31)	2.134(4)	O(2)–O(1)–Sn(1)	98.46(13)
O(1)–O(2)	1.493(3)	C(1)–O(2)–O(1)	108.60(19)
O(2)–C(1)	1.444(3)	Sn(1)–O(1)–O(2)–C(1)	-137.78(19)
3			
Pb(1)–O(1)	2.135(2)	O(1)–Pb(1)–C(21)	104.03(11)
Pb(1)–C(21)	2.191(3)	O(1)–Pb(1)–C(31)	107.11(11)
Pb(1)–C(31)	2.190(3)	O(1)–Pb(1)–C(11)	115.01(12)
Pb(1)–C(11)	2.197(3)	O(2)–O(1)–Pb(1)	101.37(15)
O(1)–O(2)	1.483(5)	C(7)–O(2)–O(1)	107.70(2)
O(2)–C(7)	1.438(4)	Pb(1)–O(1)–O(2)–C(9)	130.7(2)

X-ray powder diffraction

The triphenyltin and lead peroxocomplexes **1-3** crystals were carefully ground in a mortar. Resulting powders were placed to low background Si sample holder. Graphical representations of the Rietveld refinement results obtained for **1-3** are presented in Figure S1.

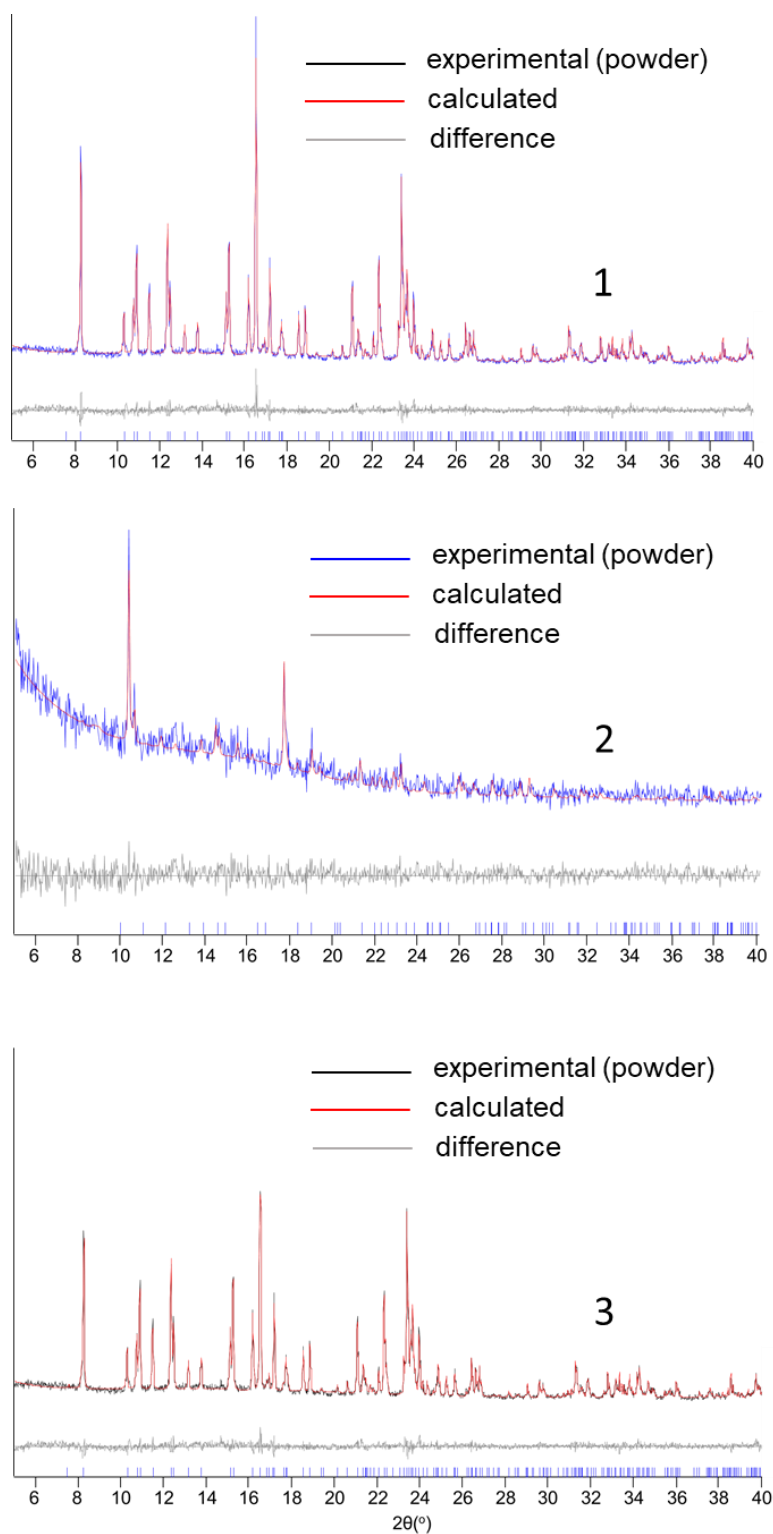


Figure S1. Rietveld refinement results for **1-3**. The vertical blue bars show the calculated positions of the Bragg reflections of **1-3**.

FTIR spectroscopy

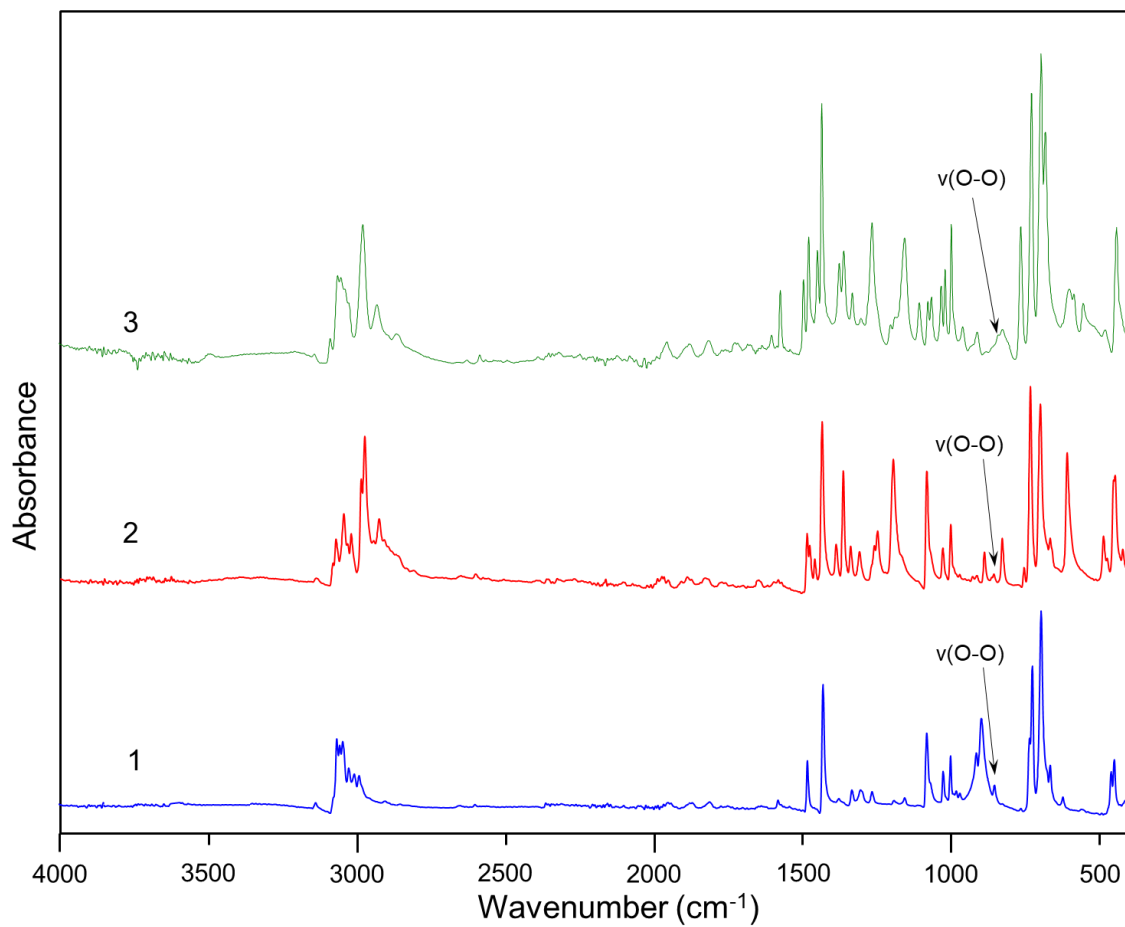


Figure S2. FTIR spectra of cumene and *tert*-butyl hydroperoxides and peroxocomplexes **1-3**.

Raman spectroscopy

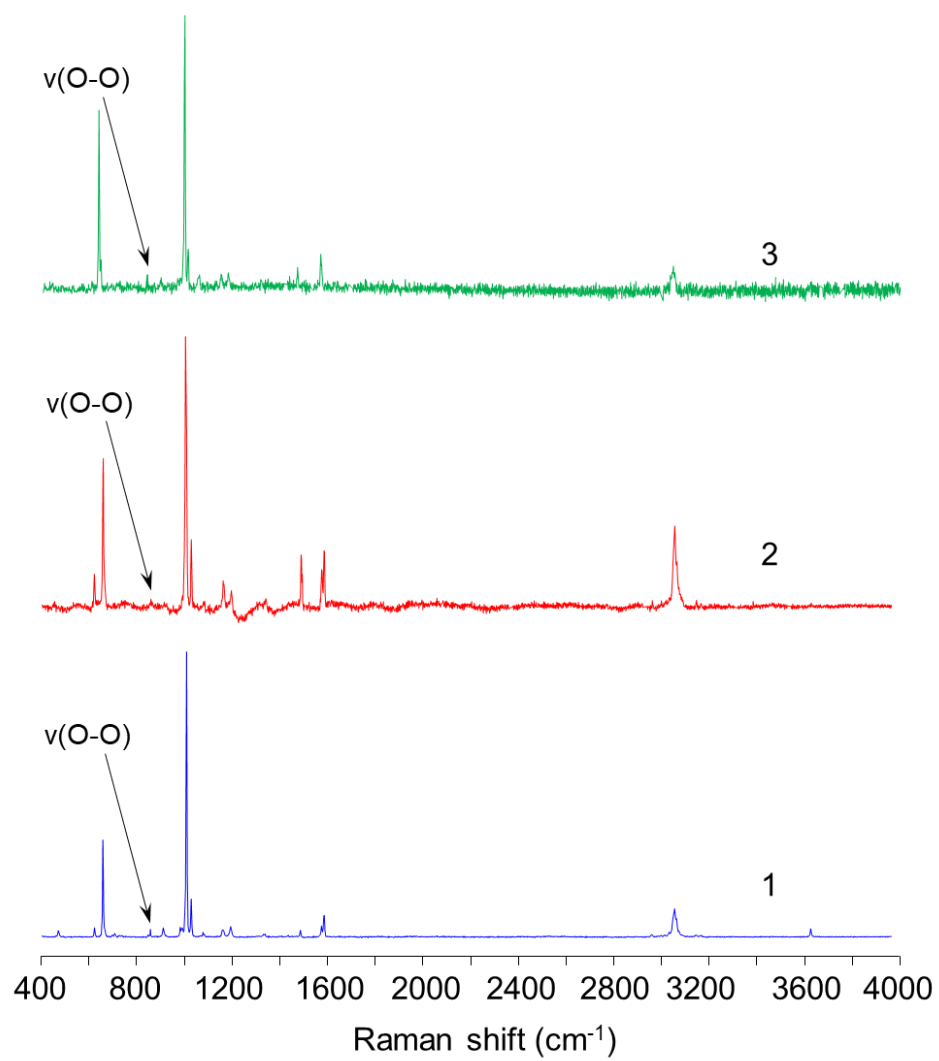


Figure S3. Raman spectra of **1-3**.

Thermal analysis

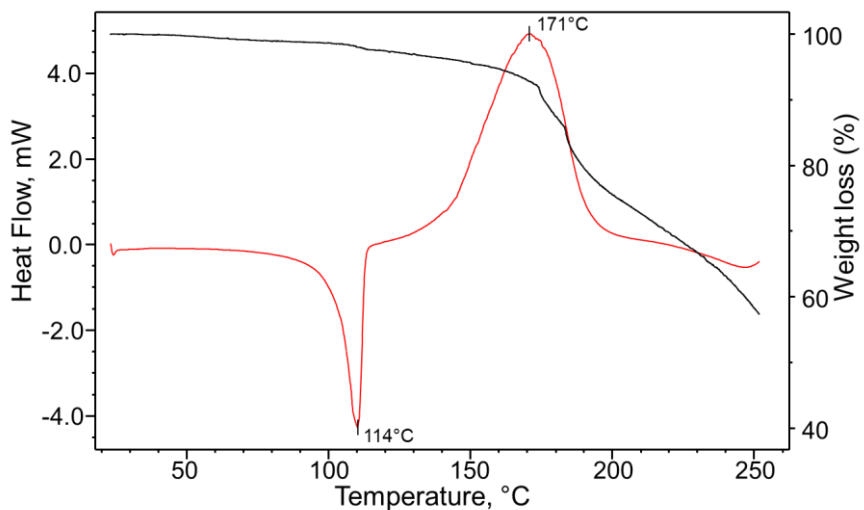


Figure S4. TGA (black) and DSC (red) curves of **1** in argon atmosphere at scan rate 5°C/min.

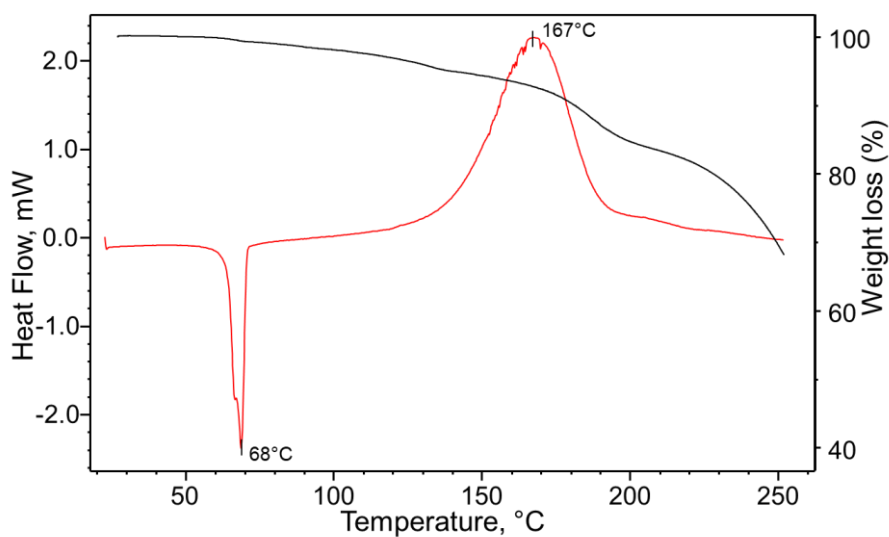


Figure S5. TGA (black) and DSC (red) curves of **2** in argon atmosphere at scan rate 5°C/min.

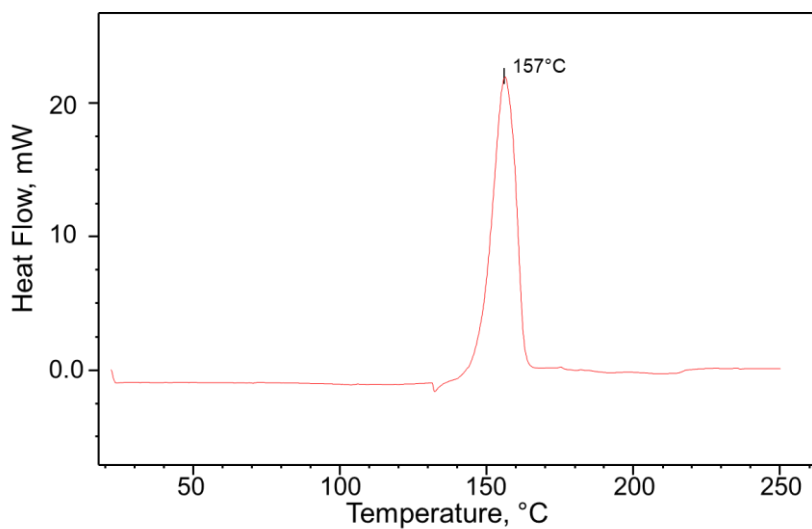


Figure S6. DSC curve of **3** in argon atmosphere at scan rate 5°C/min

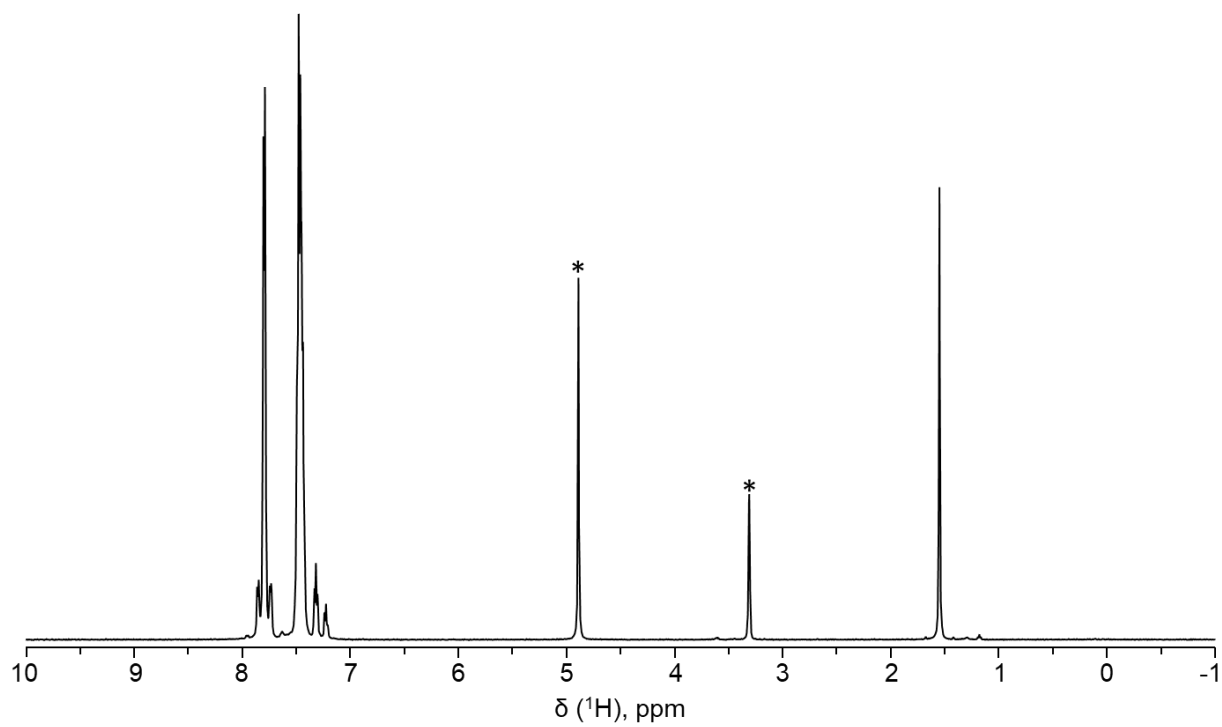


Figure S7. ^1H -NMR spectrum of **1** in CD_3OD (* solvent peaks).

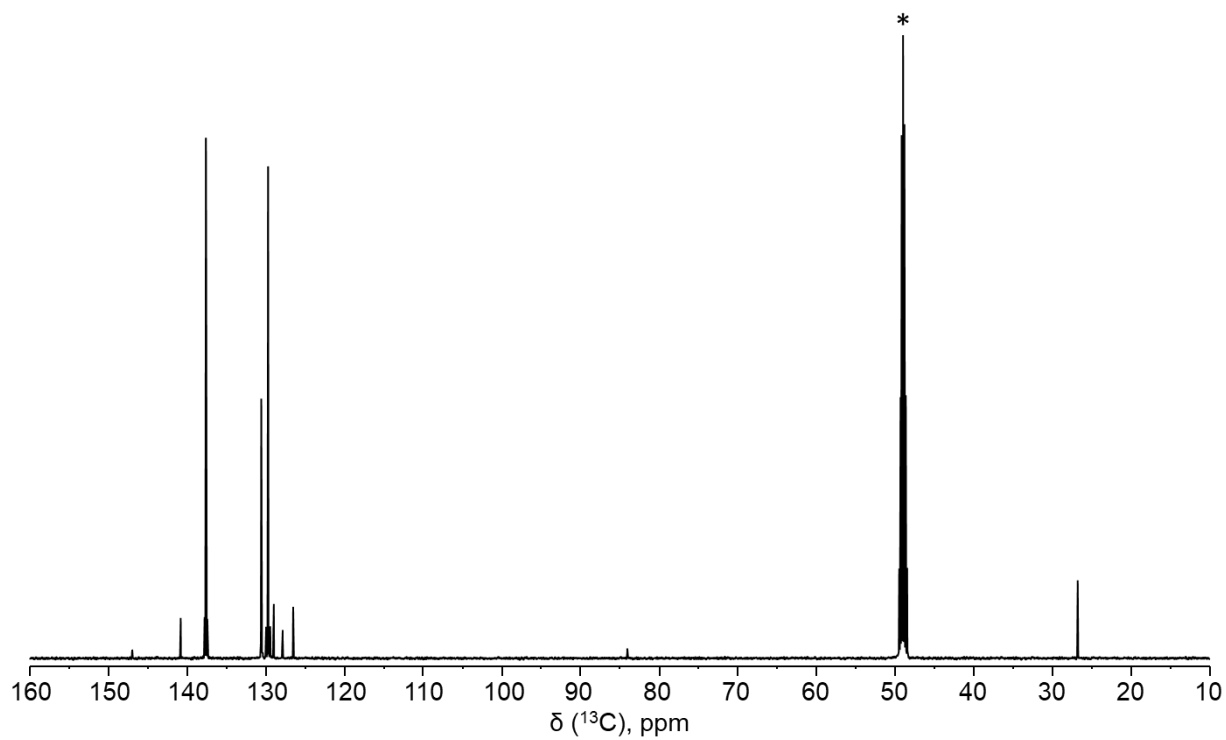


Figure S8. ^{13}C -NMR spectrum of **1** in CD_3OD (* solvent peaks).

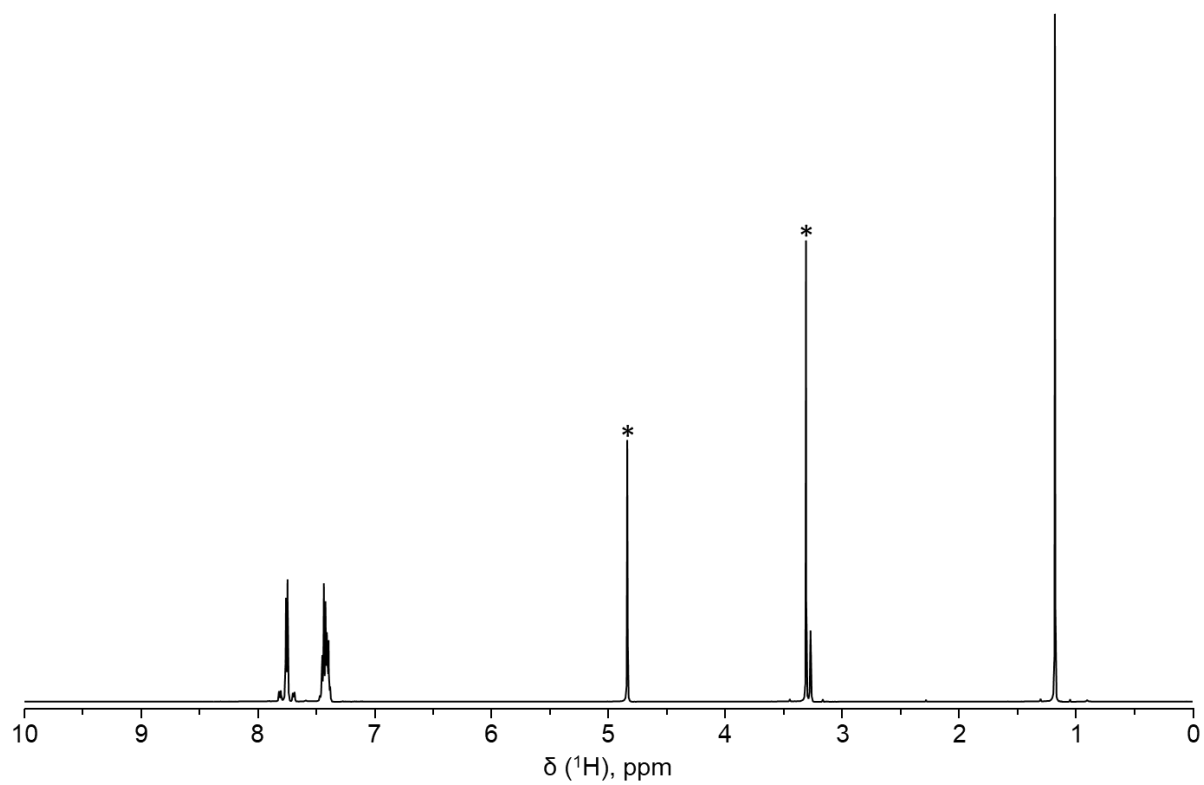


Figure S9. ^1H -NMR spectrum of **2** in CD_3OD (* solvent peaks).

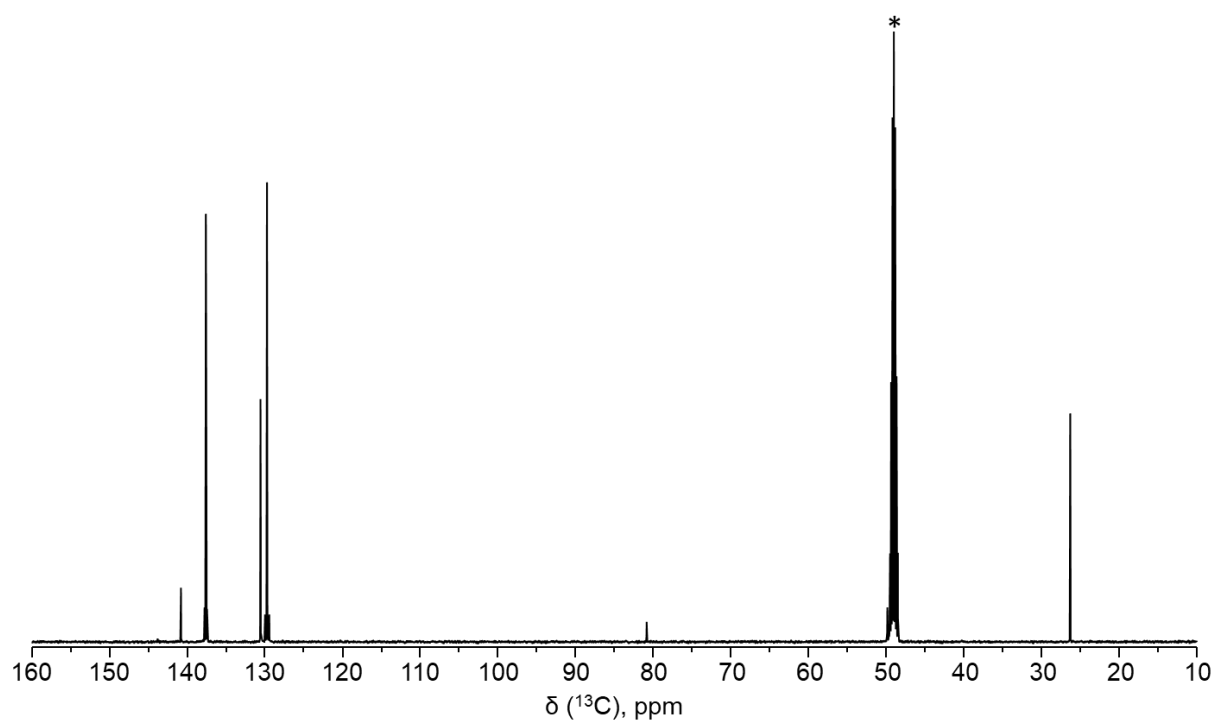


Figure S10. ^{13}C -NMR spectrum of **2** in CD_3OD (* solvent peaks).

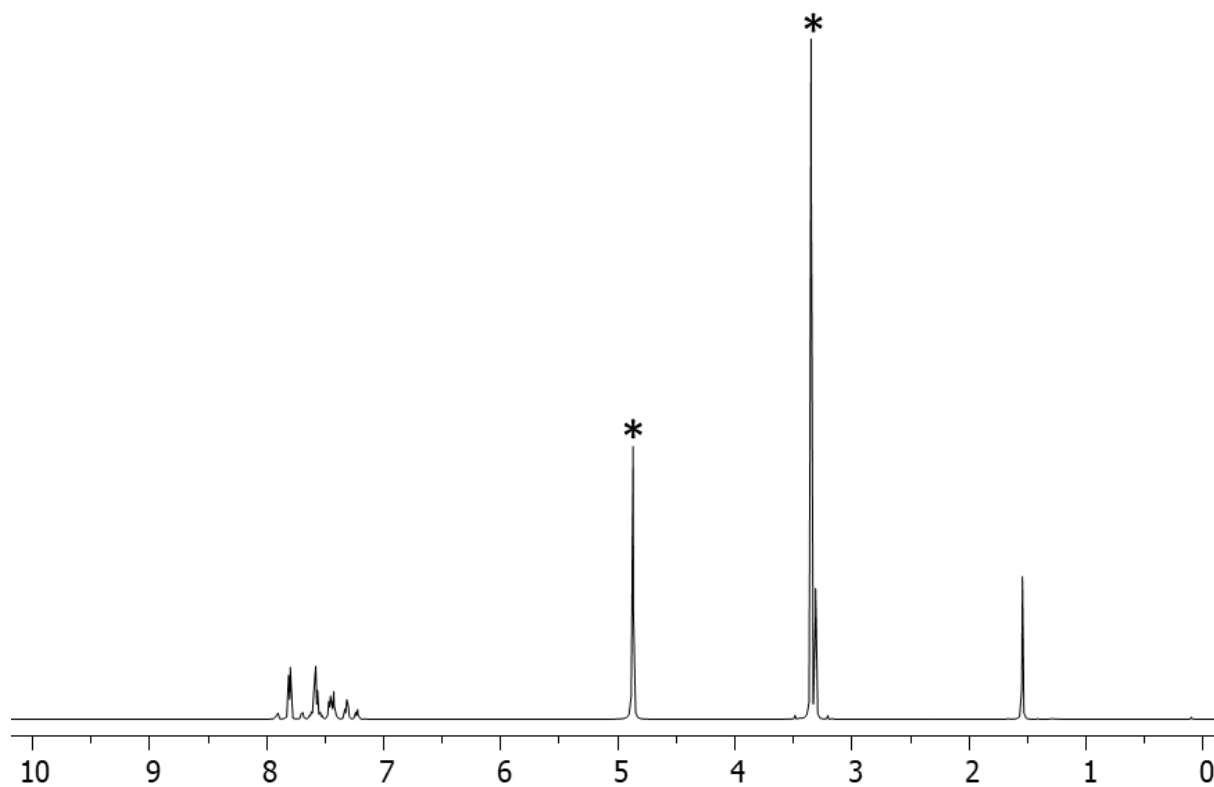


Figure S11. ^1H -NMR spectrum of **3** in CD_3OD (* solvent peaks).

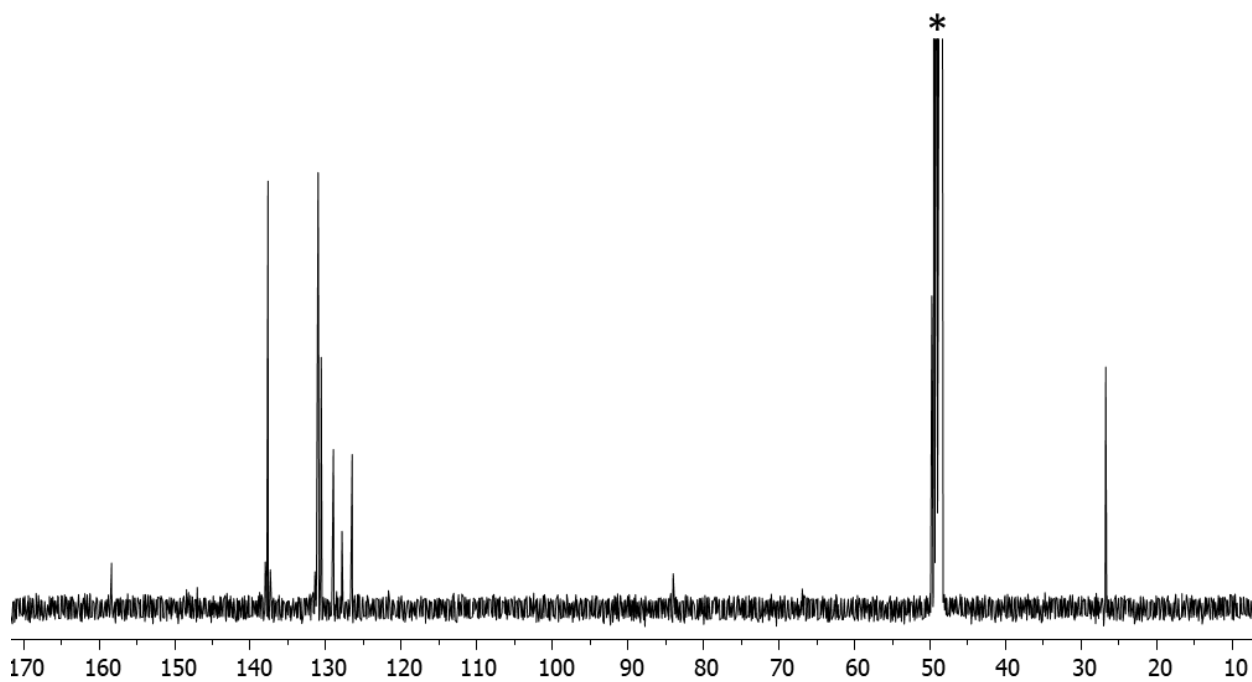


Figure S12. ^{13}C -NMR spectrum of **3** in CD_3OD (* solvent peaks).